

Long-lived Mn^{2+} emission in nanocrystalline $\text{ZnS}:\text{Mn}^{2+}$

A. A. Bol and A. Meijerink

Debye Institute, Department of Condensed Matter, Utrecht University, P.O. Box 80 000, 3508 TA Utrecht, The Netherlands

(Received 10 April 1998; revised manuscript received 3 August 1998)

Recently, it has been reported that doped semiconductor nanoparticles can yield both high luminescence efficiencies and a spectacular lifetime shortening, which suggests that doped semiconductor nanoparticles form a new class of luminescent materials for various applications. From lifetime measurements and time-resolved spectroscopy we conclude that the Mn^{2+} emission does not show a spectacular shortening of the decay time upon decreasing particle size as reported earlier. The luminescence of nanocrystalline $\text{ZnS}:\text{Mn}^{2+}$ indeed has a short decay time (~ 100 ns), but also shows a long ms range decay time. The short decay time is ascribed to a defect-related emission of ZnS, and is not from the decay of the ${}^4\text{T}_1\text{-}{}^6\text{A}_1$ transition of the Mn^{2+} impurity as suggested by other authors. The ${}^4\text{T}_1\text{-}{}^6\text{A}_1$ transition of the Mn^{2+} has a ‘‘normal’’ decay of about 1.9 ms. Based on our observations, we conclude that doped semiconductor nanoparticles do not form a new class of luminescent materials, combining a high efficiency with a short (ns) decay time. [S0163-1829(98)52048-6]

The optical properties of nanocrystalline semiconductors have been studied extensively in recent years.¹⁻⁴ These materials behave differently from bulk semiconductors. With decreasing particle size the band structure of the semiconductor changes; the band gap increases, and the edges of the bands split into discrete energy levels. These so-called quantum-confinement effects have stimulated great interest in both basic and applied research.^{5,6}

Recently, papers on the optical properties of transition-metal doped semiconductor nanoparticles have emerged. In 1994 Bhargava and Gallagher⁷ reported that doped nanocrystals of semiconductors can yield both high luminescence efficiencies and lifetime shortening from ms to ns at the same time. These spectacular results suggested that doped semiconductor nanocrystals form a new class of luminescent materials, with a wide range of application in, e.g., displays, sensors, and lasers.⁸ After the initial publication on the influence of quantum size effects on the luminescence of Mn^{2+} in ZnS, many papers from different groups have appeared on the luminescence of various doped nanocrystals and the potential application of these luminescent materials.⁹⁻¹⁹ The short decay time, in combination with a high quantum efficiency, is especially important for applications in which saturation effects limit the light output of a luminescent material (e.g., luminescent materials for projection television).

To account for the phenomena, Bhargava and Gallagher^{7,8} suggested that with decreasing particle size a strong hybridization of the s - p states of the ZnS host and the d states of the Mn^{2+} impurity should occur. This hybridization results in a faster energy transfer between the ZnS host and Mn^{2+} impurity. Due to this fast energy transfer, the radiative recombination at the Mn^{2+} impurity, which competes with nonradiative decay at the ZnS surface, becomes more efficient. This results in an increase in quantum efficiency. Also, it was argued that through this hybridization the spin-forbidden ${}^4\text{T}_1\text{-}{}^6\text{A}_1$ transition of the Mn^{2+} impurity becomes less spin forbidden, resulting in a shorter decay time.

This explanation may seem plausible at first sight, but still some doubt remains. For example, one would expect a shift of the position of the Mn^{2+} emission band due to hybridiza-

tion of the s - p states of the ZnS and d states of the Mn^{2+} impurity. This is not observed.^{7,8} Furthermore, the explanation is very qualitative and does not provide a quantitative model on how the spin-forbidden ${}^4\text{T}_1\text{-}{}^6\text{A}_1$ transition of the Mn^{2+} impurity becomes less spin forbidden through hybridization. In addition, the reported lifetime measurements are limited. Only decay times in the ns range are reported for doped nanocrystalline semiconductors. Besides the group of Bhargava, a few other groups have also reported the observation of lifetime shortening of the Mn^{2+} emission due to quantum-confinement effects. Sooklal *et al.*¹⁰ observed ns decay times in nanoclusters of $\text{ZnS}:\text{Mn}^{2+}$, while Ito *et al.*¹⁵ reported lifetime shortening to μs in two-dimensional quantum wells of $\text{ZnTe}:\text{Mn}^{2+}$. The articles on short lifetimes for the Mn^{2+} emission^{7,10,16} do not describe experiments to verify the absence of a ms decay time in nanocrystalline $\text{ZnS}:\text{Mn}^{2+}$.

In this paper we report on the ns and ms range lifetimes of the emissions of nanocrystalline ZnS doped with Mn^{2+} and investigate the origin of these ns and ms lifetimes. The $\text{ZnS}:\text{Mn}^{2+}$ nanoparticles were made by using an organometallic and an inorganic synthesis method. The organometallic method is similar to the method Gallagher *et al.*²⁰ described. In a nitrogen atmosphere (glovebox), 2.5 ml 1.1 M $\text{Zn}(\text{C}_2\text{H}_5)_2$ was dissolved in toluene. To this solution, 5 ml of a 0.011 M solution of manganecyclohexabutyrates in toluene and 1.1 ml methacrylic acid (stabilizer) were added. After adding 50 ml of a saturated solution of H_2S in toluene (0.631 M), a white suspension occurred instantaneously. The final concentration of $\text{Zn}(\text{C}_2\text{H}_5)_2$ was 0.01 M. The amount of manganese precursor used was 2% of the amount of zinc precursor used. The particles were separated from the solution by centrifuging. The separated particles were rinsed with methanol and dried in vacuo.

The inorganic synthesis route resembles standard methods for the synthesis of nanocrystalline II-VI semiconductors, and is very similar to, for example, the method described by Yu *et al.*,⁹ except that the synthesis was done in water instead of methanol. 10 ml of 1 M $\text{Zn}(\text{CH}_3\text{COO})_2 \cdot 2\text{H}_2\text{O}$,

2–10 ml of 0.1 M $\text{Mn}(\text{CH}_3\text{COO})_2 \cdot 4\text{H}_2\text{O}$ (giving a Mn^{2+} precursor percentage of 2–10 % relative to the amount of zinc precursor), and 10 g $\text{Na}(\text{PO}_3)_n$ (stabilizer) were added to 78–70 ml of distilled water. After 10 min of stirring, 10 ml of a 1 M Na_2S solution was added to the solution. Immediately after adding the Na_2S solution an opaque white fluid was obtained. After centrifuging, the particles were rinsed with distilled water and methanol and dried in vacuo.

X-ray powder diffraction patterns were recorded using a Phillips PW 1729 x-ray generator with $\text{Cu K}\alpha$ radiation ($\lambda = 1.542 \text{ \AA}$). The x-ray diffraction (XRD) pattern showed broad lines at positions that are in agreement with the zinc-blende modification of ZnS. To calculate the particle diameter from the width of the lines in the XRD spectrum, the Scherrer formula²¹ was used. According to the calculations, both synthesis methods gave nanoparticles with a diameter of approximately 4 nm, comparable to the particle size found by Bhargava⁷ and Yu.⁹

High-resolution TEM analysis was done on a Philips CM30 at 300 kV. Both an inorganic and an organic sample were suspended in ethanol and brought onto a copper grid supported with a carbon film. The TEM analysis revealed that both samples have a size distribution of 3–5 nm, the majority of the particles being 4 nm in diameter. This particle size corresponds to the particle size obtained from the XRD patterns.

Emission and excitation spectra were recorded with a SPEX Fluorolog spectrofluorometer, model F2002, equipped with 0.22 m double monochromators (SPEX 1680). Lifetime measurements were carried out using a Lambda Physik LPX 100 excimer laser (XeCl) ($\lambda_{\text{exc}} = 308 \text{ nm}$) or the fourth harmonic of a Spectra Physics DCR 2 Nd-YAG laser ($\lambda_{\text{exc}} = 266 \text{ nm}$) as an excitation source. Emission spectra at the laser setups were recorded with a Jobin-Yvon 1 m monochromator (Excimer setup) or a Spex 1269 1.26 m monochromator (YAG setup) and a Hamamatsu R928P photomultiplier (cooled to -30°C). For decay time measurements a Tektronix 2440 500 MHz digital oscilloscope was used. The time resolution of the laser setups was limited to some 50 ns by the pulse width of the lasers (20 ns) and the time resolution of the photomultiplier tube ($\sim 10 \text{ ns}$).

Time-resolved emission spectra were measured using the same experimental setups as used for the lifetime measurements, together with a gated photon counter model SR400 of Stanford Research Systems applied as a boxcar. The time delay was varied from $\sim 0 \mu\text{s}$, $3 \mu\text{s}$ to 0.5 ms with pulse widths of $2 \mu\text{s}$, $200 \mu\text{s}$, and 1 ms, respectively.

The results of the luminescence studies on the samples synthesized using the two different processing routes are shown in Fig. 1. The emission and excitation spectra are similar to the emission and excitation spectra observed by other authors.^{7,9,10} For all the samples the emission spectra show two broad emission bands, one around 420 nm and one around 590 nm. The orange emission around 590 nm can be attributed to the ${}^4\text{T}_1\text{-}{}^6\text{A}_1$ transition of the Mn^{2+} impurity. The characteristics of the orange Mn^{2+} emission are almost identical to the emission observed for Mn^{2+} in bulk ZnS. The purple/blue emission around 420 nm is also observed in undoped ZnS and can be assigned to recombination of free charge carriers at defect sites, possibly at the surface, in ZnS. This emission is not related to the Mn^{2+} impurity.

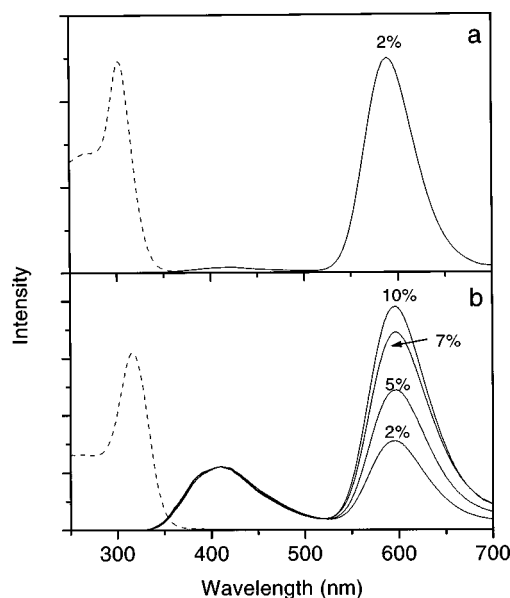


FIG. 1. The emission spectra (solid lines), recorded for $\lambda_{\text{exc}} = 300 \text{ nm}$, and excitation spectra (dashed lines), recorded for $\lambda_{\text{em}} = 590 \text{ nm}$, of nanocrystalline ZnS:Mn^{2+} made using the (a) organometallic synthesis route, and (b) inorganic synthesis route. In the figure the manganese precursor percentages relative to the amount of zinc precursor are mentioned. All spectra were recorded at 300 K.

The maximum of the excitation spectra for both samples is at approximately 300 nm. Due to quantum-confinement effects the band maximum of the excitation spectra has shifted to the blue compared with the band maximum of the excitation spectrum of bulk ZnS:Mn^{2+} which is at 332 nm.²²

Comparison of Fig. 1(a) with 1(b) shows that the emission spectra of samples with the same amounts of Mn^{2+} precursor (2% relative to Zn^{2+}) are different. The organometallic sample shows a much stronger Mn^{2+} emission band relative to the ZnS defect emission than the inorganic sample. This indicates that the amount of Mn^{2+} incorporated in ZnS is higher for the samples prepared via the organometallic synthesis route. The actual amount of Mn^{2+} incorporated in the ZnS nanoparticles has not been determined by us, but previous reports by Gallagher *et al.*²⁰ estimate that for the organometallic synthesis with 10 at. % of Mn^{2+} relative to Zn^{2+} , only 0.86 at. % of Mn is incorporated.

From Fig. 1(b) it is clear that with increasing manganese precursor percentage used for the inorganic synthesis route the Mn^{2+} emission becomes more pronounced, showing that more Mn^{2+} is incorporated in the nanocrystalline ZnS.

An interesting phenomenon, which has also been observed before,²⁰ is that the samples prepared via the organometallic synthesis route become more efficiently luminescent after UV illumination. This effect, called UV curing, causes an increase of the orange Mn^{2+} emission, as reported by Bhargava. We have observed that also the purple/blue ZnS emission increases after exposure to UV light. In fact, the ZnS emission grows more rapidly than the Mn^{2+} emission band. Although the explanation of this phenomenon is not the purpose of this paper, this observation can be explained by an UV induced polymerization of the methacrylic acid stabilizer which leads to a better surface passivation (less

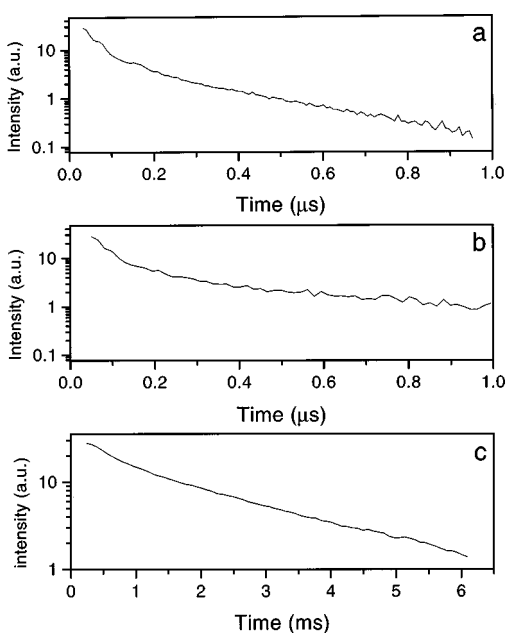


FIG. 2. Decay curves of the emissions of nanocrystalline ZnS:Mn^{2+} measured at emission wavelengths of (a) $\lambda_{\text{em}} = 400$ nm [short (ns) decay], (b) $\lambda_{\text{em}} = 600$ nm [short (ns) decay], and (c) $\lambda_{\text{em}} = 600$ nm [long (ms) decay]. The samples were excited at $\lambda_{\text{exc}} = 308$ nm (Excimer laser). All decay curves were recorded at 300 K.

nonradiative recombination at the surface), as suggested by Bhargava and Gallagher.^{7,8} Apparently, the nonradiative losses are more important in ZnS particles without Mn^{2+} , where nonradiative recombination competes with radiative recombination at defect sites (giving blue/purple emission). Due to the efficient recombination at Mn^{2+} (giving orange emission), this orange emission is less affected by nonradiative losses at surface states.

The main purpose of this paper is to verify the spectacular decrease in luminescence decay time (ms \rightarrow ns) for Mn^{2+} in nanocrystalline ZnS. To do this, the lifetime of the Mn^{2+} emission was measured in the various samples. Also, the lifetime of the purple/blue emission from ZnS was measured. Excitation was at 266 nm (YAG laser) or at 308 nm (Excimer laser). For both emissions short (ns range) and long (ms range) lifetimes were measured. The results for an inorganic sample using 308 nm excitation are shown in Figs. 2(a)–2(c). Using 266 nm excitation and for organic samples we get similar results.

The decay curve for the purple/blue emission [Fig. 2(a)] shows a multi-exponential decay with a fast initial decay ($\tau \approx 50$ ns) and a slower tail ($\tau \approx 200$ ns). The time resolution of our setup does not allow for accurate determination of the short (ns) decay times. No long ms decay can be observed. For the orange emission also, a fast multi-exponential decay ($\tau \approx 40, 250$ ns) can be observed [Fig. 2(b)]. This fast decay is similar to the fast decay reported by Bhargava and Gallagher⁷ for the orange Mn^{2+} emission. Decay time measurements for the orange Mn^{2+} emission in the ms time regime [Fig. 2(c)] show that, after an initial fast decay ($\tau \approx 0.4$ ms), a slow single exponential decay with a decay time of 1.9 ms is present. The long decay time of 1.9 ms at 600 nm is, within the experimental error, identical to

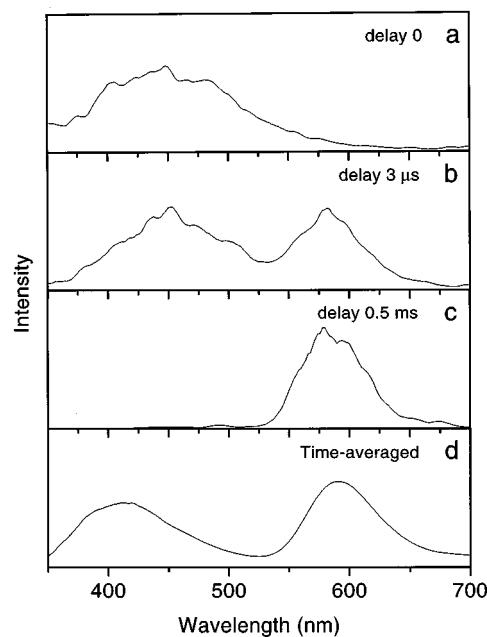


FIG. 3. Time-resolved emission spectra of nanocrystalline ZnS:Mn^{2+} . The applied time delays and gate widths are, respectively, (a) ~ 0 μs and 2 μs , (b) 3 μs and 200 μs , and (c) 0.5 ms and 1 ms. The sample was excited at 266 nm (YAG laser). In (d) the time-averaged emission spectrum ($\lambda_{\text{exc}} = 266$ nm, spectrofluorometer) of the same sample is depicted. All spectra were recorded at 300 K.

the decay time of the Mn^{2+} emission reported for bulk ZnS:Mn^{2+} (1.8 ms).²³

Based on these observations, we suspect that the short ns decay times reported before^{7,8} for the Mn^{2+} emission, are in fact due to decay of the ZnS emission. The tail of the broad purple/blue emission band extends into the region where the orange Mn^{2+} emission is located. With the setup used to measure these decay times, only short (ns) decay times can be observed due to the high repetition rate of the laser. Indeed, a short ns decay time can be observed (due to a tail of the ZnS defect emission around 590 nm), but in our opinion this is not due to Mn^{2+} emission. As far as can be deduced from the papers by Bhargava, no experiments were done to verify the absence of a long (ms) decay time by performing decay time measurements for the Mn^{2+} emission on a setup with a low repetition rate laser.

The decay time measurements reported above strongly suggest that Mn^{2+} in nanocrystalline ZnS has a ‘‘normal’’ ms decay time. Still, one can argue that the ms decay originates from a minority of Mn^{2+} ions in some large ZnS particles and that the Mn^{2+} ions in the small (4 nm) ZnS particles have a short (ns) decay time. To verify that indeed all Mn^{2+} emission in the nanocrystalline ZnS has a long ms decay time we recorded time-resolved emission spectra.

Time-resolved emission spectra were recorded for various ZnS:Mn^{2+} samples prepared via the organic and inorganic synthesis route, both for 266 nm and for 308 nm excitation. The results of a typical experiment are shown in Figs. 3(a)–3(c) for an inorganic ZnS:Mn^{2+} sample using 266 nm excitation. These time-resolved emission spectra were recorded for time delays of ~ 0 μs , 3 μs , and 0.5 ms and gate widths of, respectively, 2 μs , 200 μs , and 1 ms. For comparison, the

time-averaged emission spectrum (recorded under continuous excitation at the spectrofluorometer) of the same inorganic sample is depicted in Fig. 3(d).

The emission spectrum measured directly after the laser pulse [Fig. 3(a)] shows only the broad defect-related emission of the ZnS host at 420 nm, indicating that the ZnS related emission has a very short lifetime. When the delay is increased to 3 μ s, and the gate width is 200 μ s [Fig. 3(b)], both the 420 nm (ZnS) and the 590 nm (Mn^{2+}) emission are observed. With a delay of 0.5 ms the ZnS related emission has totally disappeared, and only the long-lived Mn^{2+} emission remains. These results support our interpretation that the ZnS emission has a short decay time (\sim 100 ns) and the Mn^{2+} emission has a "normal" decay time of about 1.9 ms, like bulk ZnS: Mn^{2+} . For 308 nm excitation, the same results as for 266 nm excitation were obtained. The relative intensities of the purple/blue and orange emission varied for the different samples (organic, inorganic, different Mn^{2+} concentrations), but in all cases the purple/blue emission dominated for short time delays and gates (\sim ns/ μ s) and only the orange emission remained in spectra recorded for long delays and gates (ms).

From the above results we conclude that the Mn^{2+} emission in nanocrystalline ZnS doped with Mn^{2+} does not show a spectacular shortening of the decay time upon decreasing particle size as reported before.^{7,8} The nanosecond decay times reported for the Mn^{2+} emission are most likely due to the tail of broad defect-related ZnS emissions which overlaps with the Mn^{2+} emission at around 590 nm. From lifetime measurements and time-resolved spectroscopy we conclude that the Mn^{2+} emission of nanocrystalline ZnS: Mn^{2+} has a decay time in the ms range, like the Mn^{2+} emission of bulk ZnS: Mn^{2+} . Therefore, doped semiconductor nanoparticles may not form the new class of luminescent materials as suggested by Bhargava and Gallagher,^{7,8} since there is not a combination of a high luminescent efficiency and a short (ns) decay time (essential in applications where saturation effects due to a long decay time are a problem). Still, efficiently luminescing doped nanoparticles can be important for other applications and the luminescence of doped nanocrystals remains an interesting field of research.

The financial support of Philips Lighting is gratefully acknowledged.

- ¹R. Rosetti, R. Hull, J. M. Gibson, and L. E. Brus, *J. Chem. Phys.* **82**, 552 (1985).
- ²L. Brus, *J. Phys. Chem.* **90**, 2555 (1986).
- ³A. Henglein, *Chem. Rev.* **89**, 1861 (1989).
- ⁴Y. Wang and N. Herron, *J. Phys. Chem.* **95**, 525 (1991).
- ⁵H. Weller, *Angew. Chem. Int. Ed. Engl.* **32**, 41 (1993).
- ⁶A. P. Alivisatos, *J. Phys. Chem.* **100**, 13 226 (1996).
- ⁷R. N. Bhargava and D. Gallagher, *Phys. Rev. Lett.* **72**, 416 (1994).
- ⁸R. N. Bhargava, *J. Lumin.* **70**, 85 (1996).
- ⁹I. Yu, T. Isobe, and M. Senna, *J. Phys. Chem. Solids* **57**, 373 (1996).
- ¹⁰K. Sooklal, B. S. Cullum, S. M. Angel, and C. J. Murphy, *J. Phys. Chem.* **100**, 4551 (1996).
- ¹¹J. Huang, Y. Yang, S. Xue, B. Yang, S. Liu, and J. Shen, *Appl. Phys. Lett.* **70**, 2335 (1997).
- ¹²M. A. Chamarro, V. Voliotis, R. Grousson, P. Lavallard, T. Gacoin, G. Couston, J. P. Boilot, and R. Cases, *J. Cryst. Growth* **159**, 853 (1996).
- ¹³E. T. Goldburt, B. Kulkarni, R. N. Bhargava, J. Taylor, and M. Libera, in *Flat Panel Display Materials II*, edited by M. Hatalis, J. Kanicki, C. J. Summers, and F. Funada, MRS Symposia Proceedings No. 424 (Materials Research Society, Pittsburgh, 1997), p. 441.
- ¹⁴Y. L. Soo, Z. H. Ming, S. W. Huang, Y. H. Kao, R. N. Bhargava, and D. Gallagher, *Phys. Rev. B* **50**, 7602 (1994).
- ¹⁵H. Ito, T. Takano, T. Kuroda, F. Minami, and H. Akinaga, *J. Lumin.* **72-74**, 342 (1997).
- ¹⁶J. Yu, H. Liu, Y. Wang, F. E. Fernandez, W. Jia, L. Sun, C. Jin, D. Li, J. Liu, and S. Huang, *Opt. Lett.* **22**, 913 (1997).
- ¹⁷T. A. Kennedy, E. R. Glaser, P. B. Klein, and R. N. Bhargava, *Phys. Rev. B* **52**, 14 356 (1995).
- ¹⁸V. Albe, C. Jouanin, and D. Bertho, *Phys. Rev. B* **57**, 8778 (1998).
- ¹⁹T. Igarashi, T. Isobe, and M. Senna, *Phys. Rev. B* **56**, 6444 (1997).
- ²⁰D. Gallagher, W. E. Heady, J. M. Racz, and R. N. Bhargava, *J. Mater. Res.* **10**, 870 (1995).
- ²¹B. D. Cullity, *Elements of X-ray Diffraction* (Addison-Wesley, Massachusetts, 1978), p. 102.
- ²²D. Gallagher, W. E. Heady, J. M. Racz, and R. N. Bhargava, *J. Cryst. Growth* **138**, 970 (1994).
- ²³H.-E. Gülich, *J. Lumin.* **23**, 73 (1981).